Magnetic Wheeled Robot with High Mobility but only 2 DOF to Control

MAGNETIC WHEELED ROBOT WITH HIGH MOBILITY BUT ONLY 2 DOF TO CONTROL

WOLFGANG FISCHER[†]
Autonomous Systems Lab, ETH Zürich, CLA E18, Tannenstrasse 3, 8092 Zürich, Switzerland,
wfischer@ethz.ch

FABIEN TÂCHE
Same group and post address, fabien.tache@mavt.ethz.ch

GILLES CAPRARI
Same group, room CLA E14.1, gilles.caprari@mavt.ethz.ch

ROLAND SIEGWART
Same group, room CLA E32, rsiegwart@ethz.ch

In this paper, the mechanical design and calculation of a magnetic wheeled climbing robot is presented. It is able to pass obstacles that previously had only been accessed by robots with more complex mechanisms, but only needs 2 actively controlled DOF. A comparison to other design alternatives and the influence of some core parameters are shown in calculations with simplified 2D models. According to these calculations, a prototype was realized to prove its functionality in real tests. The paper concludes with an outlook on further design improvements and shows possible scenarios for its industrial application in the field of power plant inspection.

1. Introduction

Robots with permanent magnetic wheels combine the simple control of wheeled robots with the high mobility of climbing robots. Compared to other attachment principles, they do not permanently need power for just staying on spot, do not need special features on the surface, and are even able to move in overhanging sections. Magnetic wheeled robots can better adapt to different curvatures than robots with magnets in the structure or magnetic tracks and do not need as many DOF as robots with magnetic legs – resulting in a simple and robust control. Due to recent advances in manufacturing technology, the formerly expensive rare-earth-magnets in ring-

[†] Work partially supported by grant KTI 8435.1 EPRP-IW of the Swiss "Bundesamt für Berufsbildung und Technologie" and ALSTOM Power Services, Baden, Switzerland.

shape (necessary for such wheels) are now widely available in almost all sizes and – compared to other components – relatively cheap.
Thus – if the environment to inspect is ferromagnetic – they are the principle of choice and are already used in many industrial applications. Most of these robots use the simplest configuration – the "tripod"-type – with 3 wheels in total, and only one or two of them motorized. For many applications in power plants [1, Fig. 2], the mobility of these robots is not high enough, as they are not able to pass obstacles like sharp diameter changes with concave corners or convex edges. In academic research, several mechanisms for such obstacles have been proposed – but not industrialized yet, as they mostly result in huge, complex or error-prone devices.
In order to propose an appropriate solution for the mentioned limitations, this paper presents a relatively simple magnetic wheeled robot – without any additional mechanisms, but with all-wheel traction, optimized geometry parameters and a simple remote control. Its functionality is both proven in calculations based on a 2D-mechanical model and in real tests with a prototype.

2. State of the art in magnetic wheeled robots

As already stated in the introduction, magnetic wheeled robots achieve several advantages towards other types of climbing robots. Thus, they are the principle of choice for several industrial applications. The two main features of these robots are the wheel design and the structure how the wheels are arranged.

2.1. *Wheel design*

The simplest and most frequently used wheel design is the one with an axially magnetized NeFeB ring magnet in the middle, two steel rims on both sides to better conduct the magnetic flux into the surface and a thin layer of rubber on the rims to increase the friction coefficient between wheel and surface from around μ=0.3 (steel/steel) up to μ=0.8. A sketch of such a wheel can be seen in many of the quoted publications, for example in [2, Fig. 3]. For improving the ratio between adhesion force and wheel mass, also other designs have been proposed, such as magnet plates close to the wheels [3]. Even if this design shows some advantages regarding the maximal payload or the rolling friction, it will not be considered further in this work, as it is more complex than the other wheel design and is not able to cope with sharp intersections as they can be typically be found at most inspection scenarios in power plants [1, Fig. 2 and 3].

2.2. *Simple vehicle structures (tripods)*

Regarding the overall structure, the simplest and most frequently used type is the "tripod"-configuration – with two motorized main wheels and one passive castor wheel for the third contact point. Examples can be found both in industrial applications such as the robot from "Jireh industries" [4] as well as in research prototypes like the one designed by the University of Strathcliffe [5]. The main advantage of this type is the easy control with only two DOF. However, their mobility is limited to plain or only slightly curved surfaces with small obstacles that are significantly smaller than the wheel radius.

2.3. *Complex vehicle structures with high mobility on specific obstacles*

For passing more difficult obstacles such as ridges, steps, concave corners and convex edges, several other vehicle structures have been developed. In order to pass these obstacles, some robots use active elements in the structure and sometimes even extra mechanisms to pull off the wheels at unwanted contact points. Examples of this type are the PipeInspectionRobot [6] or a robot for the inspection of fragile gas tanks with specifically shaped ridges [2]. These robots are able to pass very difficult types of obstacles, but result in very complex mechanisms (>8DOF) that are huge, expensive and difficult to control. For slightly less difficult obstacles that can be found in many power plant environments, the bicycle-configuration [1] was developed. This structure uses two identical wheel units with one powered wheel and one rotary lifter- and stabilization arm on each unit. Together with the actuator for steering, it totally results in 5 active DOF. It is able to pass sharp concave corners and convex edges and to adapt to small pipe diameters. However, its complexity and need for control is still much higher than for the simpler tripod-type.

3. Motivation, goal and approach

Thus, the main objective of this work is to design and analyze a robot that is as simple to control as a tripod [4; 5], but achieves an almost similar mobility as the bicycle-configuration [1].
To do so, we started with the analysis of a symmetrical four-wheeled configuration, with traction on all wheels and a simple control of only 2 DOF (= the motor speeds on the left and on the right side of the vehicle). For this configuration, we calculated its behavior on concave corners with a 2D-mechanical model and realized a prototype that was tested on this type of obstacle, on convex edges and on concave curved surfaces (pipes).
In these calculations and tests we could prove the functionality of such a configuration in passing the above specified obstacles and derive some suggestions for further design improvements.

4. Calculation of magnetic wheeled vehicles on specific obstacles

In order to better understand the behavior of magnetic wheeled vehicles on certain obstacles, at first a magnetic wheel and its forces towards the vehicle's body and the environment had to be modeled in order to derive the characterizing equations.

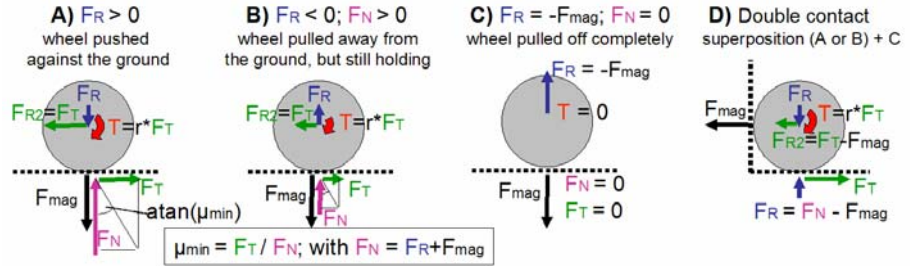

Fig. 1: Forces and torque on a magnetic wheel

As it can be seen in Fig. 1, the normal force (F_N) is not only determined by the reaction force normal to the surface (F_R), but is the sum of both this force and the magnetic attraction force ($F_N=F_R+F_{mag}$). Thus, the wheel still sticks to the surface and is able to provide traction, even if the reaction force (F_R) gets negative (wheel pulled, Fig. 1, B). The limit case is reached, when the reaction force pulls as strong as the magnetic force (Fig. 1, C). When a wheel is in contact with two surfaces, the two cases can be superposed. To estimate if the vehicle is able to move, two factors are crucial:

- The actuator torque ($T=r*F_T$) has to be high enough to provide the necessary traction force (F_T). This is normally not the biggest problem, but has of course taken into consideration for the actuator choice in the design.
- The necessary friction coefficient ($\mu_{min}=F_T/F_N$) that is determined by the traction force (F_T) and the normal force (F_N) has to be below the maximal obtainable value of μ. This value can be measured by placing the wheel (or the entire vehicle) on a non-magnetic plate with similar surface characteristics and change the inclination of this plate until the wheel starts to slip. With normal rubber, values between 0.5 and 0.8 can be achieved. Without rubber, only a value of around 0.3 can be achieved.

4.1. *Model of a vehicle that is passing a concave corner*

Starting from these basic equations, we simulated the behavior of a vehicle with two wheel pairs passing a concave corner. As it was already shown in [1], the two worst cases always occur when one wheel is in contact with two surfaces. In both cases, the vehicle needs very huge traction forces (F_T) to get rid of the unwanted magnetic force (F_{mag}) towards the old surface. The mechanical model for both cases and the corresponding equation system is shown in Fig. 2.

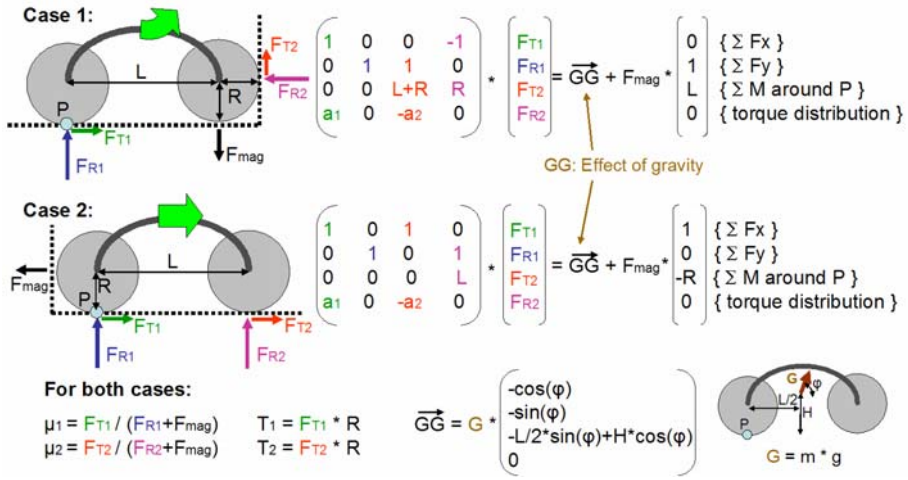

Fig. 2: 2D-model of a magnetic wheeled vehicle in concave corners

From this model we derived the corresponding force- and moment-equilibriums. These equations, together with a 4th one for the torque distribution between front and back wheels were put together into one matrix equation and solved in MATLAB.

4.2. *Simplified calculation without the effect of gravity*

In order to roughly estimate if a vehicle as described in the previous section can pass or not, and to point out the advantages of all-wheel-traction; the first calculation was done with a simplified model that does not take into account the gravity (G=m*g=0). Note that with this simplification, the values for μ_{min} are independent of F_{mag} and φ and only depend on two parameters: The ratio between length and wheel radius (L/R) and the torque distribution between front and back wheel ($F_{T1}/F_{t2}=a_2/a_1$).

Table 1: Necessary friction coefficient in both wheels (μ_{min1}; μ_{min2}) for a magnetic wheeled vehicle that is passing a concave corner, without the effect of gravity

$\mu_{min} < 0.5$ $0.5 <= \mu_{min} < 0.75$ $0.75 <= \mu_{min}$	Case 1; L=3R	Case 2; L=3R	Case 1; L=5R	Case 2; L=5R
Front wheel traction ($F_{T1} = 0$)	(0) 0.75	(0) 1.5	(0) 0.833	(0) Back wheel 1.25 Front wheel
Back wheel traction ($F_{T2} = 0$)	1.5 (0)	0.75 (0)	2.5 (0)	0.833 Back wheel (0) Front wheel
Equal torque in both wheels ($F_{T1} = F_{T2}$)	0.429 0.375	0.375 0.75	0.556 0.417	0.417 Back wheel 0.625 Front wheel
Equal friction in both wheels ($\mu_1 = \mu_2$)	0.396 (0.396)	0.5 (0.5)	0.464 (0.464)	0.5 Back wheel (0.5) Front wheel

Estimating a realistic friction coefficient of $\mu_{real} \approx 0.5$ - 0.75 between wheel and surface, this simplified calculation already shows the following:

- Vehicles with only one motorized wheel pair cannot pass concave corners.
- Vehicles with all-wheel traction are able to pass, if the gravity force (G=m*g) resulting from the vehicle's mass (m) is significantly lower than the magnetic force (F_{mag}).

5. Mechanical design of a simple test prototype

In order to experimentally prove and analyze in detail the above mentioned results; we built a simple test prototype. It consists of two identical wheel units that are powered by DC-Motors with planetary gearboxes (T=2Nm each motor) and connected to the magnetic wheels with a gear belt transmission. These gear belts can easily be removed to also test the vehicle with traction on only one wheel pair. For the wheels, we used a NeFeB ring magnet (Ø15,Ø30*8) with two steel rims (Ø15,Ø40*10 → R=20mm) and a cover of 5 layers of isolation tape to increase the friction. With these wheels, we measured an adhesion force of 45N each wheel (→ F_{mag}=90N for one unit) and a friction coefficient of around $\mu_{real} \approx 0.6$. The mass of the total vehicle was measured 1.5 kg, which results in a gravity force of G=m*g=15N=F_{mag}/6. The distance between the wheels was set to L=100mm=5*R. The center of mass is approximately at H=40mm.

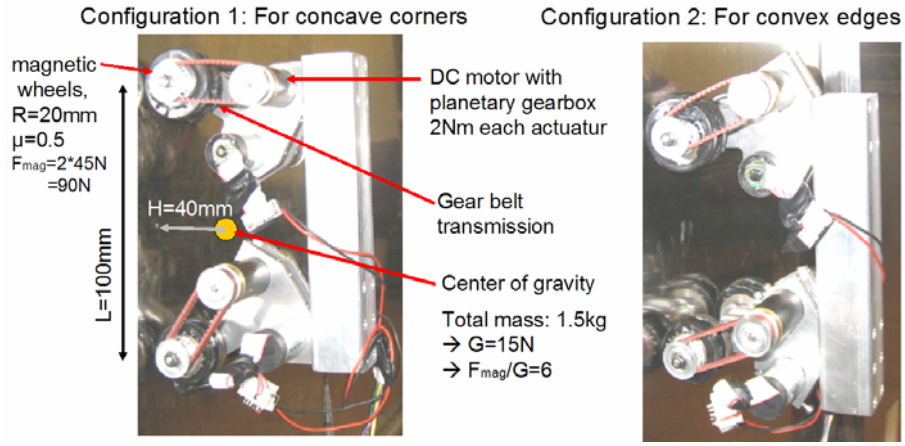

Fig. 3: The test prototype and its basic mechanical properties

For steering with only two DOF, both left and both right motors are connected to the same cable. The cables of both sides are connected to a power supply with constant voltage and controlled by the user with "on-off-on" switches. In order to also do tests on convex edges, the vehicle can be assembled in a slightly different way that offers enough ground clearance for this type of obstacle (Fig. 3, right).

6. Tests and comparison to the calculation results

With this prototype we tested its obstacle-passing capability on concave corners and compared these results to our calculation – this time taking into account the effect of gravity ($G=6*F_{mag}$ for this test prototype).
Additionally, we also successfully tested the obstacle-passing capability on convex edges and the ability to turn on spot with skid-steering – both on flat ground and in a pipe with small inner diameter.

6.1. *Tests on concave corners and comparison to calculation results*

The calculation was done for both cases and in all possible inclinations (φ = 0°-360°); the tests only in 4 (φ =0°, 90°, 180°, 270°). Both results are represented in Fig. 4, with the charts showing the calculation and with the points the tests.

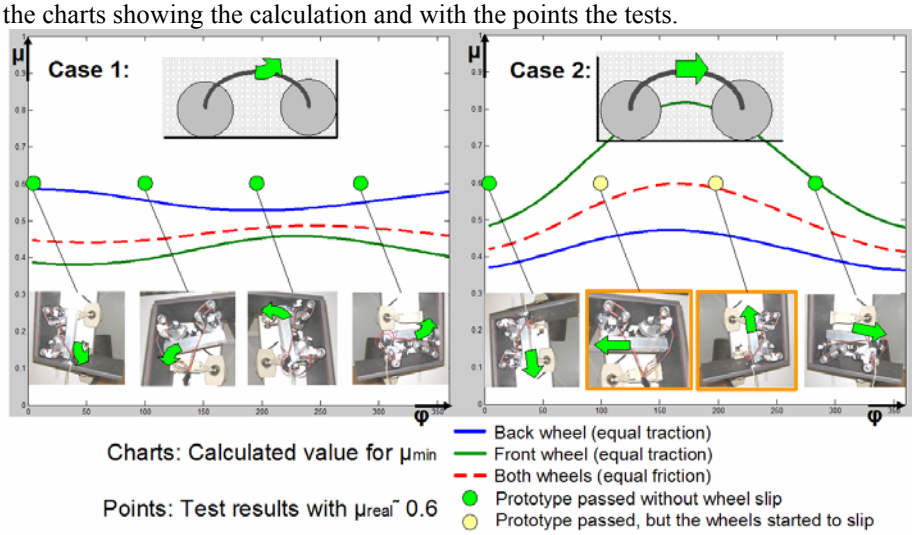

Fig. 4: Calculation and test results for concave corners

In these tests, the prototype passed the concave corner in all inclinations. In most cases, this was even without slip in the wheels. Only in the two worst cases (marked in yellow), the wheels started to slip. This observation well correlates with the calculation and allows for better interpreting the charts of μ_{min}; and for estimating the behavior of vehicles that are controlled with similar voltage on the motors for both wheel pairs, resulting in equal torque on both wheels.

- If the real friction coefficient (μ_{real}) is above all charts for μ_{min}, the vehicle can pass without slip.
- If it is between the highest chart and the chart for equal friction in both wheels (Fig. 5, dashed red chart), it can still pass but the wheels start to slip.

This effect can be interpreted as follows: When a wheel starts slipping, the traction force (F_T) is decreased and shifts to the value that was calculated for the case of equal friction in both wheels.

- If the real friction coefficient (μ_{real}) is below the red chart, the vehicle should not be able to pass any more. This case was not tested yet, but seems consequential.

6.2. *Other tests with the prototype*

Aside from the calculations and tests on concave corners, we also tested the behavior on convex edges and the ability to turn with simple skid steering – both on flat surfaces and on the inner surfaces of pipes with small diameter (D=250mm).

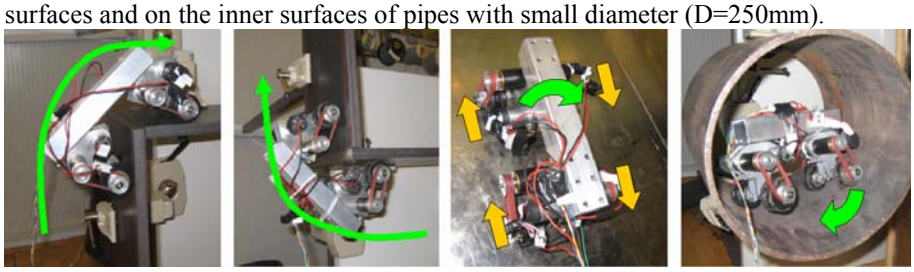

Fig. 6: Other tests with the prototype: Convex edges, turning on flat surfaces and in pipes

There we obtained the following results:

- The passage of convex edges worked well in most cases. Only when these edges were extremely sharp and we did not approach them in a right angle, the robot sometimes fell down. This limitation should be improved in the next version, where we plan to add an additional free joint that will assure the contact of all 4 wheels at any time.
- Turning on flat surfaces worked without any problem. However, a precise odometry can very likely not be achieved, as the exact slip in the wheels cannot be determined well.
- Turning in pipes resulted to be slightly more difficult, but also worked well. Note that in this case always one wheel is lifted off the ground. Adding a free joint as already mentioned before will also help in this case. As the pipe was very rusty, the rubber got slightly damaged.

7. Conclusion and outlook to further work

Both the calculations and the real tests showed, that the here proposed vehicle structure – despite its simplicity – is able to pass several types of obstacles such as concave corners and convex edges; and to turn in small pipe curvatures. Thus, it should be able to move in many environments that can be encountered in power plants, such as steam chests, boiler pipes and complex shaped storage tanks; and form a robust locomotion platform for carrying many types of inspection sensors.

The simple control of only 2 DOF does not only bring significant advantages in terms of cost and reliability, it also allows to build the mechanism at very small size - for accessing very narrow environments that have not even been considered for robotic inspection before.
However, the obstacle-passing capability is only limited to rather clean environments where a good friction coefficient of approximately $\mu_{real} \geq 0.6$ can always be assured and where the obstacles are well separated from each other. If this is not the case, a more complex vehicle structure (like [1]) still seems to be required.
Future work will mainly stress on the following work packages:

- Further optimization of the existing prototype - with better wheels ($\mu_{real} \approx 0.8$; more robust on rusty surfaces), a free joint between the wheel units for a better adaptation to the ground, enough ground clearance to pass both types of obstacles without changing the configuration, a camera and an interface for inspection sensors.
- Further tests to estimate the maximum allowed payload on the above described obstacles and field tests in real environments.
- Derivation of a downsized version (expected size: 50x50x30mm), to access very narrow environments.

References

1. F. Tache, W. Fischer, R. Siegwart, R. Moser, F. Mondada, *Compact Magnetic Wheeled Robot With High Mobility for Inspecting Complex Shaped Pipe Structures*, Proc. of The IEEE/RSJ International Conference on Intelligent Robots and Systems (IROS), 2007
2. W. Fischer, F. Tache, R. Siegwart, *Magnetic Wall Climbing Robot for Thin Surfaces with Specific Obstacles*, Proc. of The 6th International Conference on Field and Service Robotics (FSR), 2007
3. K. Liu, W. Zhang, P. Zeng, *Symmetrically centralized magnetic-wheel unit for wall-climbing robots*, Proc. of the 13th IASTED International Conference Robotics and Applications, Würzburg, 2007
4. URL http://www.jireh-industries.com, Jireh Industries LTD., 2008
5. M. Friedrich, L. Gatzoulis, G. Hayward and W. Galbraith, *Small Inspection Vehicles for Non-Destructive Testing Applications*, Proc. of The 8th International Conference on Climbing and Walking Robots and the Support Technologies for Mobile Machines (CLAWAR 2005), part 17, pages 927-934, 2005
6. T. Yukawa, H. Okano, S. Komatsubara, *Mechanisms for the movement of piping inspection robot with magnetic elements*, Proc, of the IASTED International Conference Robotics and Applications, Cambridge, USA525390, 2005